Towards efficient analysis of postbuckling in aircraft stiffened structures

Elalfy, Mohamed H.; de Breuker, Roeland; Castro, Saullo G.P.

Publication date
2024

Document Version
Final published version

Published in
34th Congress of the International Council of the Aeronautical Sciences, ICAS 2024

TOWARDS EFFICIENT ANALYSIS OF POSTBUCKLING IN AIRCRAFT STIFFENED STRUCTURES

Mohamed H. Elalfy[1], Roeland de Breuker[2] & Saullo G. P. Castro[3]

[1]Ph.D. Candidate, Faculty of Aerospace Engineering, Delft University of Technology, m.h.i.elalfy@tudelft.n
[2]Associate Professor, Faculty of Aerospace Engineering, Delft University of Technology, r.debreuker@tudelft.nl
[3]Associate Professor, Faculty of Aerospace Engineering, Delft University of Technology, s.g.p.castro@tudelft.nl

Abstract

This paper introduces a new computationally efficient tool to predict the postbuckling behavior of thin-walled aircraft structures, particularly stiffened panels. Focusing on the critical transition where local buckling alters load distribution but retains the structure's load-carrying capacity, the proposed postbuckling analysis method employs a semi-analytical Rayleigh-Ritz-based model and the perturbation approach. The assumed geometrically compatible displacement field functions are based on hierarchical polynomials, which are able to enhance the versatility and computational efficiency of the semi-analytical model, enabling its application across a wider range of structural configurations and boundary conditions, whereas currently available perturbation-based methodologies are limited to simple boundary conditions. The enhancement in computational efficiency, additionally, provides substantial benefits to the design and optimization processes. The obtained results for the linear case perfectly match the analytical values for buckling load. For the nonlinear case, results come in a good agreement with literature.

Keywords: Postbuckling, perturbation approach, semi-analytical, hierarchical polynomials

1. Introduction

Thin-walled aircraft structures are highly expected to experience instability as a dominant failure mode [1]. A typical airframe is made of multiple elements which may undergo instability separately or collectively, in what is known as local buckling or global buckling, respectively. The aircraft structures are mainly stiffened plates reinforced by ribs and stiffeners. Stiffened plates are more likely to buckle locally between ribs and stiffeners, but they will still be able to carry load after buckling [1]. When a panel buckles locally, its local stiffness is reduced reflecting a reduction in the load carrying capacity of the skin region, with load being distributed to the adjacent stiffeners. Many methodologies have been developed in the literature to predict the behaviour of post-buckled stiffened panels. Grisham [2] introduced a methodology to predict the postbuckling behaviour of metallic panels, in a method based on prestrain loading instead of stiffness reduction of elements. The method required a detailed mesh of different structural components, making it computationally expensive. A program called VICONOPT [3] was first developed to design plate assemblies subject to buckling constraints. Then, Anderson [4] extended the program to allow postbuckling below the design load. He accounted for the reduction in stiffness by multiplying the initial stiffness by a factor of half. Collier and Yarrington [5] modeled the reduction in the stiffness due to postbuckling using the effective width method and disregarding the region that assumed to no longer carry load. As an example of the efforts done under the supervision of the project POSICOSS is the simulation developed by Mocker and Reimerdes [6], based on strip elements to reduce the number of degrees of freedom and consequently the computational time. Trigonometric functions were used as a basis for the displacement field to describe simply supported stiffened panels. The problem they reported, is the need of many terms to capture the postbuckling behavior, which in turn increases the computational cost. Moreover, the use of

sine trigonometric functions to represent the out-of-plane deflections limited their work to simply supported panels. Different approaches of predicting the postbuckling behaviour based on metamodels consisting of response surfaces have been developed [7, 8], but still limited by the design space and specific load cases that were used to train the metamodels.
The present study proposes a new method for analyzing postbuckling, using a Rayleigh-Ritz-based semi-analytical model and the perturbation approach. The distinctive feature of the proposed method involves utilizing hierarchical polynomials instead of traditional trigonometric shape functions. This development not only improves the flexibility of the model in handling various boundary conditions, but also uses the recurrence nature of Legendre polynomials to derive closed-form integrals, thereby reducing the dependence on numerical integration and significantly enhancing computational efficiency. The proposed tool holds promise in providing a practical solution for predicting postbuckling behavior in stiffened plates, making it adaptable to a broader range of structural configurations in the realm of aircraft design and optimization.

1.1 Implementation

The formulation starts with assuming a displacement field that is capable of keeping the four edges of the plate straight in the deformed state, as shown in Fig. 1:

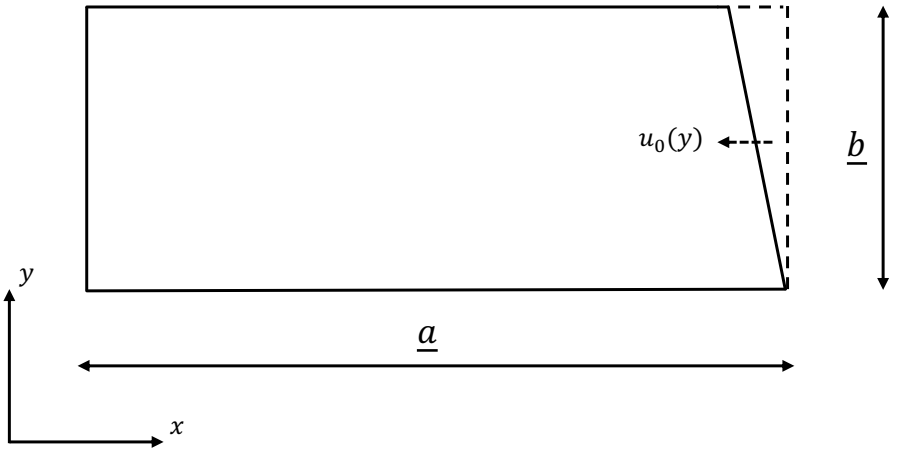

Figure 1 – Plate under applied edge strain only in the x direction

$$
\begin{aligned}
w(x,y) &= \sum_{i=1}^{N} a_i \phi_i^w \\
u(x,y) &= -\lambda e_{x0} x - \lambda \frac{g_{xy0}}{2} y + \sum_{i=1}^{2N} b_i \phi_i^u, \quad \text{and} \\
v(x,y) &= -\lambda e_{y0} y - \lambda \frac{g_{xy0}}{2} x + \sum_{i=1}^{2N} c_i \phi_i^v
\end{aligned}
\tag{1}
$$

Seresta et al. [9] employed trigonometric shape functions which limited their analysis to simply supported plates. Here, hierarchical Legendre polynomials are used, which are defined as:

$$
\begin{aligned}
\phi_i^u &= L_m(\zeta) L_n(\eta) \\
\phi_i^v &= L_m(\zeta) L_n(\eta) \\
\phi_i^w &= H_m(\zeta) H_n(\eta)
\end{aligned}
\tag{2}
$$

where L_i represents Lobatto Polynomials and H_i represents the integral of the Lobatto Polynomials, both expressed as follows:

$$\begin{aligned} L_{i+1}(\xi) &= \int_{-1}^{\zeta} P_i(\xi)d\zeta, \quad i \geqslant 1 \\ H_{i+1}(\zeta) &= \int_{-1}^{\zeta} L_i(\zeta)d\zeta, \quad i \geq 3 \end{aligned} \tag{3}$$

where P_i represents Legendre Polynomials.
The nonlinear strains are described assuming the von Kármán model in terms of mid-plane strains and curvatures:

$$\varepsilon_x = \varepsilon_x^0 + z\kappa_x, \quad \varepsilon_y = \varepsilon_y^0 + z\kappa_y, \quad \text{and} \quad \gamma_{xy} = \gamma_{xy}^0 + z\kappa_{xy} \tag{4}$$

where:

$$\begin{aligned} &\varepsilon_x^0 = u_{,x} + \frac{1}{2}w_{,x}^2, \quad \varepsilon_y^0 = v_{,y} + \frac{1}{2}w_{,y}^2, \quad \gamma_{xy}^0 = u_{,y} + v_{,x} + w_{,x}w_{,y}, \\ &\kappa_x = -w_{,xx}, \quad \kappa_y = -w_{,yy}, \quad \kappa_{xy} = -2w_{,xy} \end{aligned} \tag{5}$$

then the total potential energy is evaluated:

$$\begin{aligned} \Pi(u,v,w) = \frac{1}{2}\int_0^{\underline{a}}\int_0^{\underline{b}} \Big[& A_{11}\left(\varepsilon_x^0\right)^2 + 2A_{12}\varepsilon_x^0\varepsilon_y^0 + A_{22}\left(\varepsilon_y^0\right)^2 \\ & + A_{66}\left(\gamma_{xy}^0\right)^2 + D_{11}\kappa_x^2 + 2D_{12}\kappa_x\kappa_y + D_{22}\kappa_y^2 + D_{66}\kappa_{xy}^2 \Big] \, \mathrm{d}x \, \mathrm{d}y \end{aligned} \tag{6}$$

The recurrence nature of Legendre polynomials is used to find a closed form for the integrals instead of using numerical integration which is supposed to increase the computational efficiency. The next step is to minimize the total potential energy with respect to Ritz coefficients leading to the following equilibrium equations:

$$\begin{aligned} & -g_l^u + K_{il}^{ub}b_i + K_{il}^{uc}c_i + K_{ijl}^{uaa}a_ia_j = 0 \\ & -g_l^v + K_{il}^{vb}b_i + K_{il}^{vc}c_i + K_{ijl}^{vaa}a_ia_j = 0 \\ & K_{il}a_i - \lambda\bar{K}_{il}^{g}a_i + K_{ikl}^{wba}b_ia_k + K_{ikl}^{wca}c_ia_k + K_{ijkl}^{waaa}a_ia_ja_k = 0 \end{aligned} \tag{7}$$

where:

$$\begin{aligned} g_l^u &= g_l^{ux}e_{x0} + g_l^{uy}e_{y0} + g_l^{uxy}g_{xy0} \\ g_l^v &= g_l^{vx}e_{x0} + g_l^{vy}e_{y0} + g_l^{vxy}g_{xy0} \\ \bar{K}_{il}^{g} &= \bar{K}_{il}^{gx}e_{x0} + \bar{K}_{il}^{gy}e_{y0} + \bar{K}_{il}^{gxy}g_{xy0} \end{aligned} \tag{8}$$

and the definitions of the tensors are given in the appendix.

Solving for the in-plane Ritz coeffecients from the first two equations, and then substituting in the third equation, leads to the general non-linear equilibrium equation:

$$\left[K_{il} - \lambda K_{il}^{g}\right]a_i + K_{ijkl}^{\mathrm{NL}}a_ia_ja_k = 0 \tag{9}$$

where the definitions of the tensors are given in the appendix.

The nonlinear equilibrium equation depends on uniform strains and Ritz coefficients. These parameters can be expanded into series using the perturbation approach.

$$\begin{aligned} e_{x0} &= e_{x0}^{(0)} + \varepsilon^2 e_{x0}^{(2)} + \cdots \qquad e_{y0} = e_{y0}^{(0)} + \varepsilon^2 e_{y0}^{(2)} + \cdots \\ g_{xy0} &= g_{xy0}^{(0)} + \varepsilon^2 g_{xy0}^{(2)} + \cdots \quad a_i = \varepsilon a_i^{(1)} + \varepsilon^3 a_i^{(3)} + \cdots \end{aligned} \tag{10}$$

Substituting eqn 10 back into non-linear equilibrium equation 9 then equating coefficients of different powers of ε to zero, results in multiple equations. The equation corresponding to the power of ε, gives the linear buckling eigen value problem from which critical buckling loads and modes can be assessed. The coefficient of ε^3 gives another equation that is used to calculate the second-order perturpation coefficients of the average applied strains. The approximate postbuckling stiffness can be determined by evaluating the ratios of the second-order perturpation coefficients of the in-plane stress resultants to the average in-plane strains.

2. Results

A simply supported laminate of $[(0\ 90)_4]_s$ stacking sequence, and ($\underline{a} = 10in$ and $\underline{b} = 10in$) dimensions is studied. The material properties are given in table 1.

Table 1 – Ply properties

E_{11}[psi]	E_{22}[psi]	G_{12}[psi]	v	t_{ply}[in]
18.5×10^6	1.6×10^6	0.832×10^6	0.35	0.005

2.1 Linear Buckling Analysis

The results of the linear buckling analysis is obtained by solving the linear eigenvalue problem:

$$\left[K_{il} - \left(K_{il}^{gx} e_{x_0}^{(0)} + K_{il}^{gy} e_{y_0}^{(0)} + K_{il}^{gxy} g_{xy_0}^{(0)}\right)\right] a_i^{(1)} = 0 \tag{11}$$

As a verification, the obtained results –for a panel under loading only in x-direction– were compared to the analytical buckling value, with the error calculated as a percentage:

$$\text{Error}(\%) = \frac{\left|Ncr_{\text{numerical}} - Ncr_{\text{analytical}}\right|}{Ncr_{\text{analytical}}} * 100 \tag{12}$$

The result shown in Fig. 2 shows that the error falls below 1 % after using 12 terms in the Ritz expansion.

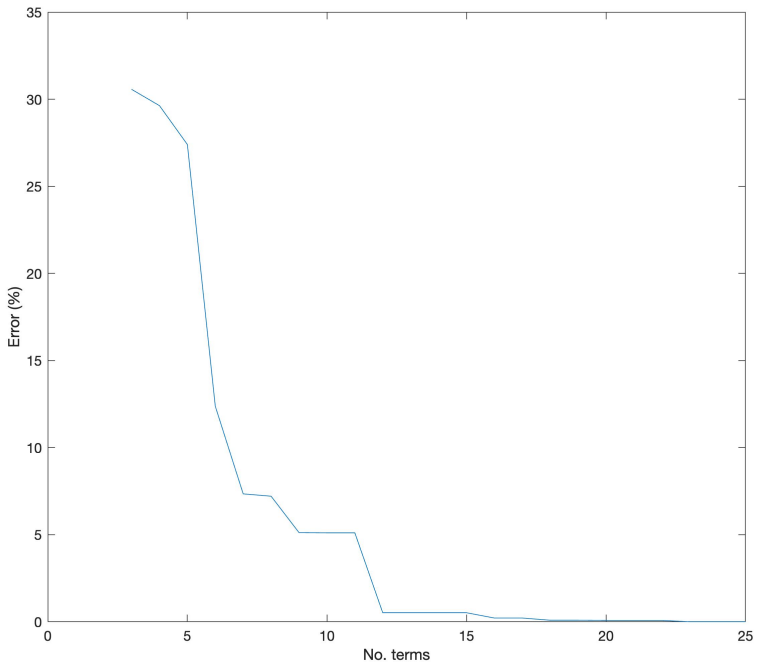

Figure 2 – Error percentage vs. No. of terms used in Ritz formulation

2.2 Nonlinear Analysis

In this part an estimate for the postbuckling stiffness is introduced. This is done by expanding the average resultant forces using the perturbation approach [9] as follows:

$$\begin{aligned} \bar{N}_x &= \bar{N}_x^{(0)} + \varepsilon^2 \bar{N}_x^{(2)} + \cdots \\ \bar{N}_y &= \bar{N}_y^{(0)} + \varepsilon^2 \bar{N}_y^{(2)} + \cdots \\ \bar{N}_{xy} &= \bar{N}_{xy}^{(0)} + \varepsilon^2 \bar{N}_{xy}^{(2)} + \cdots \end{aligned} \tag{13}$$

The postbuckling stiffnesses can then be estimated as the ratios between the second order perturbed parameters of average resultant loads over average strains as follows:

$$A_{11}^{\mathrm{PB}} = \frac{\bar{N}_x^{(2)}}{e_{x0}^{(2)}}; \quad A_{12}^{\mathrm{PB}} = \frac{\bar{N}_x^{(2)}}{e_{y0}^{(2)}}; \quad A_{21}^{\mathrm{PB}} = \frac{\bar{N}_y^{(2)}}{e_{x0}^{(2)}}; \quad A_{22}^{\mathrm{PB}} = \frac{\bar{N}_y^{(2)}}{e_{y0}^{(2)}}; \quad A_{66}^{\mathrm{PB}} = \frac{\bar{N}_{xy}^{(2)}}{g_{xy0}^{(2)}} \tag{14}$$

The average loads over the displaced edges in the postbuckling regime are calculated and will be compared to the results from literature [9]. The following formula is used to evaluate the average loads:

$$\begin{aligned} N_x &= \frac{1}{\underline{b}} \int_0^{\underline{b}} N_x(\underline{a}, y)\mathrm{d}y \\ N_y &= \frac{1}{\underline{a}} \int_0^{\underline{a}} N_y(x, \underline{b})\mathrm{d}x \end{aligned} \tag{15}$$

Table 2 – Results Comparison

				Full Analysis		Seresta et. al		Current Method	
Laminate lay up	u_0/v_0	λ_{cr}	λ^f	N_x	N_y	N_x	N_y	N_x	N_y
$[(0\ 90)_4]_S$	$(1/0)\times 10^{-3}$	1.22	13.96	711.5	-294.5	767.6	-303.61	768.9	-384.3
$[(0\ 90)_4]_s$	$(1/1)\times 10^{-3}$	0.61	8.29	244.8	239.07	268.96	268.96	228.4	228.4

The results are reported in table 2 where a comparison is done between the current formulation, the full nonlinear analysis and the results from [9]. Results are evaluated for two different loading conditions where u_0/v_0 represents the type of strain applied at the edge, λ_{cr} represents the critical multiplier for buckling, and λ^f represents the full load multiplier at which the results are assessed.

It is clear that the error is higher for N_y which was noticed also in the work of [9]. They reported an error that can reach up to 100% in some cases especially when u_0 is larger than v_0 as in the first loading condition. It was explained in [9] that the relatively large errors in N_y is not crucial for the design process as it can be considered as a secondary loading direction. In cases where u_0 is comparable to v_0, the error goes very low as in the second loading condition in which the error does not exceed 7%.

3. Conclusion and Future Work

This study presents a computationally efficient postbuckling analysis method for thin-walled aircraft structures using a semi-analytical Rayleigh-Ritz-based model and perturbation approach. By utilizing hierarchical polynomials, our method avoids numerical integration and handles a wider range of boundary conditions compared to similar methods in literature.
Our results, both linear and nonlinear, align well with established literature, confirming the accuracy and reliability of the proposed method. This validation highlights the method's potential for practical application in aerospace design and optimization.

For future work, we suggest extending the analysis to a wider variety of cases, including different dimensions, stacking sequences, boundary conditions, and loading conditions. This would further demonstrate the robustness and applicability of our method across diverse scenarios, enhancing its utility in practical aerospace design and optimization.

4. Contact Author Email Address

The contact author email address is: m.h.i.elalfy@tudelft.nl

5. Copyright Statement

6. Acknowledgment

We would like to extend our gratitude to Pedro Higino Cabral and Alex Pereira do Prado at Embraer for their help and innovative ideas, which significantly contributed to this project. Our regular meetings and discussions were invaluable to our research.

References

[1] J. Singer, Johann. Arbocz, and T. Weller. *Buckling experiments : experimental methods in buckling of thin-walled structures*. Wiley, 1998.

[2] Andrew F. Grisham. METHOD FOR INCLUDING POST-BUCKLING OF PLATE ELEMENTS IN THE INTERNAL LOADS ANALYSIS OF ANY COMPLEX STRUCTURE IDEALIZED USING FINITE ELEMENT ANALYSIS METHODS. pages 359–369. AIAA, 1978.

[3] F. W. Williams, D. Kennedy, M. S. Anderson, and R. Butler. VICONOPT - Program for exact vibration and buckling analysis or design of prismatic plate assemblies. *AIAA Journal*, 29(11):1927–1928, 1991.

[4] M. S. Anderson. Design of panels having postbuckling strength. In *Collection of Technical Papers - AIAA/ASME/ASCE/AHS/ASC Structures, Structural Dynamics and Materials Conference*, volume 3, pages 2407–2413. AIAA, 1997.

[5] Craig Collier, Phil Yarrington, and Barry Van West. Composite, grid-stiffened panel design for post buckling using Hypersizer®. In *Collection of Technical Papers - AIAA/ASME/ASCE/AHS/ASC Structures, Structural Dynamics and Materials Conference*, volume 1, pages 157–172, 2002.

[6] Torsten Möcker and Hans Günther Reimerdes. Postbuckling simulation of curved stiffened composite panels by the use of strip elements. *Composite Structures*, 73(2):237–243, 5 2006.

[7] R. Rikards, H. Abramovich, K. Kalnins, and J. Auzins. Surrogate modeling in design optimization of stiffened composite shells. *Composite Structures*, 73(2):244–251, 5 2006.

[8] Luca Lanzi and Vittorio Giavotto. Post-buckling optimization of composite stiffened panels: Computations and experiments. *Composite Structures*, 73(2):208–220, 5 2006.

[9] Omprakash Seresta, Mostafa M. Abdalla, and Zafer Gürdal. Approximate internal load prediction in composite structures with locally buckled panels. *Journal of Aircraft*, 45(2):513–522, 2008.

Appendix (Tensors Definitions)

Tensors in equation 9 are expanded as follows:

$$K_{il}^{g} = \bar{K}_{il}^{g} - \begin{bmatrix} K_{lip}^{wba} & K_{lip}^{wca} \end{bmatrix} (K^{a})_{ps}^{-1} \begin{Bmatrix} g_{s}^{u} \\ g_{s}^{v} \end{Bmatrix}$$

$$K_{lkji}^{\mathrm{NL}} = K_{lkji}^{waaa} - \begin{bmatrix} K_{lkp}^{wba} K_{lkp}^{wca} \end{bmatrix} (K^{a})_{ps}^{-1} K_{sji}^{uvaa}$$

where:

$$[K^{a}] = \begin{bmatrix} \begin{bmatrix} K^{ub} \end{bmatrix} & \begin{bmatrix} K^{uc} \end{bmatrix} \\ \begin{bmatrix} K^{vb} \end{bmatrix} & \begin{bmatrix} K^{vc} \end{bmatrix} \end{bmatrix} \tag{16}$$

The full tensors definitions are defined here. Starting by first order tensors:

$$g_{l}^{ux} = \int_{0}^{\underline{a}} \int_{0}^{\underline{b}} A_{11} \phi_{l,x}^{u} \, \mathrm{d}x \, \mathrm{d}y$$

$$g_{l}^{uy} = \int_{0}^{\underline{a}} \int_{0}^{\underline{b}} A_{12} \phi_{l,x}^{u} \, \mathrm{d}x \, \mathrm{d}y$$

$$g_{l}^{uxy} = \int_{0}^{\underline{a}} \int_{0}^{\underline{b}} A_{66} \phi_{l,y}^{u} \, \mathrm{d}x \, \mathrm{d}y$$

$$g_{l}^{vx} = \int_{0}^{\underline{a}} \int_{0}^{\underline{b}} A_{12} \phi_{l,y}^{v} \, \mathrm{d}x \, \mathrm{d}y$$

$$g_{l}^{vy} = \int_{0}^{\underline{a}} \int_{0}^{\underline{b}} A_{22} \phi_{l,y}^{v} \, \mathrm{d}x \, \mathrm{d}y$$

$$g_{l}^{vxy} = \int_{0}^{\underline{a}} \int_{0}^{\underline{b}} A_{66} \phi_{l,x}^{v} \, \mathrm{d}x \, \mathrm{d}y$$

Second order tensors:

$$K_{il}^{ub} = \int_{0}^{\underline{a}} \int_{0}^{\underline{b}} \left[A_{11} \phi_{i,x}^{u} \phi_{l,x}^{u} + A_{66} \phi_{i,y}^{u} \phi_{l,y}^{u} \right] \mathrm{d}x \, \mathrm{d}y$$

$$K_{il}^{uc} = \int_{0}^{\underline{a}} \int_{0}^{\underline{b}} \left[A_{12} \phi_{i,y}^{v} \phi_{l,x}^{u} + A_{66} \phi_{i,x}^{v} \phi_{l,y}^{u} \right] \mathrm{d}x \, \mathrm{d}y$$

$$K_{il}^{vb} = \int_{0}^{\underline{a}} \int_{0}^{\underline{b}} \left[A_{12} \phi_{i,x}^{u} \phi_{l,y}^{v} + A_{66} \phi_{i,y}^{u} \phi_{l,x}^{v} \right] \mathrm{d}x \, \mathrm{d}y$$

$$K_{il}^{vc} = \int_{0}^{\underline{a}} \int_{0}^{\underline{b}} \left[A_{22} \phi_{i,y}^{v} \phi_{l,y}^{v} + A_{66} \phi_{i,x}^{v} \phi_{l,x}^{v} \right] \mathrm{d}x \, \mathrm{d}y$$

$$\bar{K}_{il} = \int_{0}^{\underline{a}} \int_{0}^{\underline{b}} \left[D_{11} \phi_{i,xx}^{w} \phi_{l,xx}^{w} + D_{12} \phi_{i,yy}^{w} \phi_{l,xx}^{w} + D_{12} \phi_{i,xx}^{w} \phi_{l,yy}^{w} + D_{22} \phi_{i,yy}^{w} \phi_{l,yy}^{w} + 4 D_{66} \phi_{i,xy}^{w} \phi_{l,xy}^{w} \right] \mathrm{d}x \, \mathrm{d}y$$

$$\bar{K}_{il}^{gx} = \int_{0}^{\underline{a}} \int_{0}^{\underline{b}} \left[A_{11} \phi_{i,x}^{w} \phi_{l,x}^{w} + A_{12} \phi_{i,y}^{w} \phi_{l,y}^{w} \right] \mathrm{d}x \, \mathrm{d}y$$

$$\bar{K}_{il}^{gy} = \int_{0}^{\underline{a}} \int_{0}^{\underline{b}} \left[A_{12} \phi_{i,x}^{w} \phi_{l,x}^{w} + A_{22}^{v} \phi_{i,y}^{w} \phi_{l,y}^{w} \right] \mathrm{d}x \, \mathrm{d}y$$

$$\bar{K}_{il}^{gxy} = \int_{0}^{\underline{a}} \int_{0}^{\underline{b}} \left[A_{66} \phi_{i,y}^{w} \phi_{l,x}^{w} + A_{66} \phi_{i,x}^{w} \phi_{l,y}^{w} \right] \mathrm{d}x \, \mathrm{d}y$$

Third order tensors:

$$K_{ijl}^{uaa} = \frac{1}{2} \int_{0}^{\underline{a}} \int_{0}^{\underline{b}} \left[A_{11} \phi_{i,x}^{w} \phi_{j,x}^{w} \phi_{l,x}^{u} + A_{12} \phi_{i,y}^{w} \phi_{j,y}^{w} \phi_{l,x}^{u} + A_{66} \phi_{i,x}^{w} \phi_{j,y}^{w} \phi_{l,y}^{u} + A_{66} \phi_{i,y}^{w} \phi_{j,x}^{w} \phi_{l,y}^{u} \right] \mathrm{d}x \, \mathrm{d}y$$

$$K_{ijl}^{vaa} = \frac{1}{2} \int_{0}^{\underline{a}} \int_{0}^{\underline{b}} \left[A_{12} \phi_{i,x}^{w} \phi_{j,x}^{w} \phi_{l,y}^{v} + A_{22} \phi_{i,y}^{w} \phi_{j,y}^{w} \phi_{l,y}^{v} + A_{66} \phi_{i,x}^{w} \phi_{j,y}^{w} \phi_{l,x}^{v} + A_{66} \phi_{i,y}^{w} \phi_{j,x}^{w} \phi_{l,x}^{v} \right] \mathrm{d}x \, \mathrm{d}y$$

$$K_{ikl}^{wba} = \int_{0}^{\underline{a}} \int_{0}^{\underline{b}} \left[A_{11} \phi_{i,x}^{u} \phi_{k,x}^{w} \phi_{l,x}^{w} + A_{12} \phi_{i,x}^{u} \phi_{k,y}^{w} \phi_{l,y}^{w} + A_{66} \phi_{i,y}^{u} \phi_{k,y}^{w} \phi_{l,x}^{w} + A_{66} \phi_{i,y}^{u} \phi_{k,x}^{w} \phi_{l,y}^{w} \right] \mathrm{d}x \, \mathrm{d}y$$

$$K_{ikl}^{wca} = \int_{0}^{\underline{a}} \int_{0}^{\underline{b}} \left[A_{12} \phi_{i,y}^{v} \phi_{k,x}^{w} \phi_{l,x}^{w} + A_{22} \phi_{i,y}^{v} \phi_{k,y}^{w} \phi_{l,y}^{w} + A_{66} \phi_{i,x}^{v} \phi_{k,y}^{w} \phi_{l,x}^{w} + A_{66} \phi_{i,x}^{v} \phi_{k,x}^{w} \phi_{l,y}^{w} \right] \mathrm{d}x \, \mathrm{d}y$$

Fourth order tensor:

$$\bar{K}^{waa}_{ijkl} = \frac{1}{2}\int_0^a \int_0^b \left[A_{11}\phi^w_{i,x}\phi^w_{j,x}\phi^w_{k,x}\phi^w_{l,x} + A_{12}\phi^w_{i,y}\phi^w_{j,y}\phi^w_{k,x}\phi^w_{l,x} + A_{12}\phi^w_{i,x}\phi^w_{j,x}\phi^w_{k,y}\phi^w_{l,y} + A_{22}\phi^w_{i,y}\phi^w_{j,y}\phi^w_{k,y}\phi^w_{l,y} \right.$$
$$\left. + A_{66}\phi^w_{i,x}\phi^w_{j,y}\phi^w_{k,y}\phi^w_{l,x} + A_{66}\phi^w_{i,x}\phi^w_{j,y}\phi^w_{k,x}\phi^w_{l,y} + A_{66}\phi^w_{i,y}\phi^w_{j,x}\phi^w_{k,y}\phi^w_{l,x} + A_{66}\phi^w_{i,y}\phi^w_{j,x}\phi^w_{k,x}\phi^w_{l,y}\right] \mathrm{d}x\ \mathrm{d}y$$